The 3D mixed-dimensional quench model of a high aspect ratio high temperature superconducting coated conductor tape

W.K. Chan[1,2*], P. Masson[3], C. Luongo[4], J. Schwartz[2]
[1]Department of Mechanical Engineering, FAMU-FSU College of Engineering, Tallahassee, FL, USA
[2]Department of Materials Science and Engineering, North Carolina State University, Raleigh, NC, USA
[3]Advanced Magnet Lab, Palm Bay, FL, USA
[4]ITER Organization/Magnet Division in Saint Paul-lez-Durance, France
*Corresponding author: wchan@ncsu.edu

Abstract: A successful development of an effective quench detection and protection method for a high temperature superconducting (HTS) coil based on a HTS coated conductor tape lays on a thorough understanding of its slowly propagating, 3D quench behavior. Toward this goal, a 3D micrometer scale FE thermo-magnetostatic HTS tape model composed of laminated high aspect ratio thin layers is developed. The physics from all layers are accounted for in real dimensions. The modeling problem of laminated high aspect ratio thin layers is tackled effectively by using a weak-form, mixed-dimensional modeling approach through the use of interior boundaries. The interior boundaries also served as a bridge coupling the 2D and 3D physics. This also efficiently addresses the convergence problem in solving a FE model composed of domains with vastly different material properties. The model is validated numerically and experimentally; results show that it is capable of reproducing physical quench behavior accurately.

Keywords: Superconducting coated conductor, high aspect ratio thin layer, quench modeling, mixed-dimensional, finite element.

1. Introduction

Commercially available high temperature superconducting (HTS) coated conductors (CCs) such as YBCO CCs are able to transport high critical current density (J_c) at high temperature above 40K or in very high magnetic field at 4.2 K. They have been used to build superconducting motor and high field magnets. A typical HTS CC is composed of laminated thin layers. The HTS thin film, typically of 1 μm thick, is grown on a relatively thick substrate and the HTS-substrate composite layer is surrounded by a stabilizer layer typically of copper. Silver and buffer thin films of about a few μm thick are grown between the HTS and stabilizer and HTS and substrate, respectively. See Figure 1 and Figure 2 for a longitudinal and transverse cross-sectional, schematic view of a surround-stabilizer tape. When a local temperature rise created in a HTS coil is high enough to turn the superconductor from superconducting state to normal state, the transport current flowing in the HTS layer redistributes to the stabilizer in which Joule heating occurs. In case the initial heated region is large enough to generate enough Joule heating to sustain a growing normal zone with increasing temperature, quench eventually happens. Temperature margins of systems using HTS CCs are very high and therefore such systems are very stable. Even though quench-inducing instabilities are unlikely, they remain a possibility and are difficult to detect. As the operating temperature increases, thermal diffusivity becomes very low leading to very slow normal zone propagation velocity (NZPV). As a result, conventional approaches to quench detection, which are typically based upon monitoring voltages and temperatures, are impractical and either new detection methods and/or ways to increase the NZPV are needed. Therefore, it is paramount to understand quench propagation at the micrometer-scale level.

Here a 3D high-fidelity CC tape model composed of laminated, high aspect ratio layers is developed by using a mixed-dimensional modeling approach. The model takes into account all material layers in actual dimensions and is implemented in COMSOL. The main feature of the 3D mixed-dimensional approach is that the high aspect-ratio, superconducting thin film is approximated by 2D tangential equations and discretized with regular, second-order surface Lagrange finite elements. Corrective equations are added to compensate for the loss of accuracy due to the reduction in dimension. The coupling of the 2D physics to the 3D physics is done through the implementation of contact

resistance type interior boundary conditions which also model the silver layer and buffer layers analytically as normal fluxes. Another important benefit of this approach is that the interior boundary conditions simplify the computation of a model composed of different domains with vastly different material properties.

2. Mixed-dimensional 3D/2D Tape Model

Only a few superconductivity models [1, 2] address the thin film modeling issues directly. However, they are difficult to be extended to this work, which involves the study of current distribution in a 3D domain consisting of laminated thin films with nonlinear physics. Here the goal is to investigate quench behavior of a CC transporting a direct current. Due to the spatial symmetrical/anti-symmetrical behavior of the thermal and current fields along the tape length and tape width, only a quarter of the tape is modeled, see Figure 1 and Figure 2. To initiate a quench, a heater is installed on the left-end top surface of the tape, as shown in Figure 1.

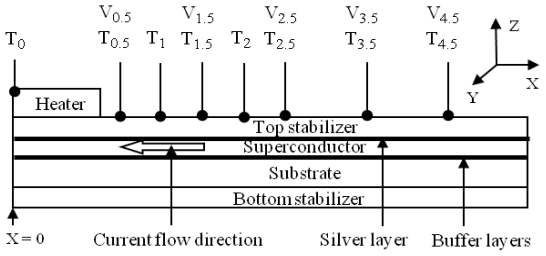

Figure 1. Longitudinal cross-sectional sketch of a half-length surround-stabilizer tape. Also shown are the voltage and temperature taps used in experimental validation. The subscripts of the tap names denote the distance (in cm) from the left end (x=0).

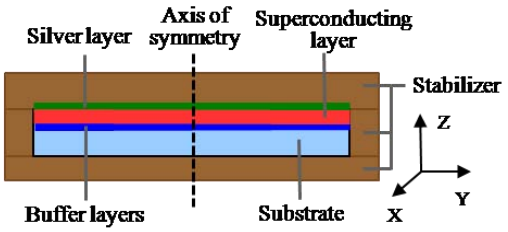

Figure 2. Transverse cross-sectional sketch of a surround-stabilizer tape. Only half of the tape width along the axis of symmetry is needed for modeling.

In view of the slow normal zone propagation velocity, the slowly changing magnetic field is ignored by dropping the time derivative term of the magnetic potential, thereby decoupling the magnetic and electric potentials in Maxwell equations. The electrical equations for a full 3D tape model are then

$$\nabla\cdot(-\sigma_\alpha(T)\nabla V)=0 \tag{1}$$

$$\mathbf{J}=\sigma_\alpha(\mathbf{E},T)\mathbf{E} \tag{2}$$

$$\mathbf{E}=-\nabla V\,. \tag{3}$$

For a tape composed of non-magnetic material, the magnetic equation is

$$\nabla\times\frac{1}{\mu_0}\nabla\times\mathbf{A}=\mathbf{J} \tag{4}$$

and the thermal equation is

$$\rho_\alpha(T)C_\alpha(T)\frac{\partial T}{\partial t}+\nabla\cdot(-K_\alpha(T)\nabla T)=Q \tag{5}$$

$$Q(T)=\mathbf{J}\cdot\mathbf{E}\,. \tag{6}$$

Here V is the electric potential, T is the absolute temperature, $\mathbf{J}$ is the current density, $\mathbf{E}$ is the electric field, $\mathbf{A}$ is the magnetic vector potential and Q is the Joule heating. Here $\alpha\in\{cu,ni,S\}$, where "cu" represents the copper stabilizer, "ni" represents the nickel-alloy substrate and "S" represents the superconducting layer. The conductivity of the superconducting layer is derived from the nonlinear E-J power law as

$$\sigma_S(\mathbf{E},T)=J_c(T,\mathbf{B})\frac{\|\mathbf{E}\|^{\frac{1-n}{n}}}{E_c^{\frac{1}{n}}}+\sigma_0 \tag{7}$$

where the critical electric field $E_c=10^{-4}$ V/m and n is the E-J power law index. σ_0 is a small constant used to ease convergence. The field and temperature dependent critical current density J_c is

$$J_c(T,\mathbf{B})=J_c(T)\frac{B_0}{\|\mathbf{B}\|+B_0} \tag{8}$$

$$J_c(T)=\begin{cases}J_{co}\left(\dfrac{T_c-T}{T_c-T_o}\right)^{\beta} & \text{if } T<T_c,\\ 0 & \text{if } T\ge T_c.\end{cases} \tag{9}$$

Here J_{co} is the critical current density at the operating temperature T_o, T_c is the critical temperature and β is the power index in the J-T relation. B_0 is a material dependent constant. The initial conditions are $T(t=0)=T_o$ and $V(t=0)=0$, which is enforced by null initial applied current. The boundary conditions are shown in Tables 1 and 2 (refer to Figure 1), where J_a is the normal

component of an applied current, and h_e and h_b are the heat transfer coefficients for cooling at the end and base of the tape, respectively. The magnetic boundary condition for the magnetic air region is magnetic insulation.

Table 4.1. Electrical boundary conditions

Boundary	Condition
Left end	Ground ($V = 0$)
Right end	Inflow current ($-\sigma_S \nabla V \cdot \mathbf{n} = J_a$)
All others	Insulation ($\nabla V \cdot \mathbf{n} = 0$)

Table 4.2. Thermal boundary conditions

Boundary	Condition
Bottom	Heat flux ($K\nabla T \cdot \mathbf{n} = h_b (T_0 - T)$)
Right end	Heat flux ($K\nabla T \cdot \mathbf{n} = h_e (T_0 - T)$)
All others	Insulation ($\nabla T \cdot \mathbf{n} = 0$)

By first separating the normal component (z-component) in the thermal equation (5) for the superconducting layer and then integrating the resulted equation over the superconducting layer thickness one obtains

$$d_S \rho_S(\tilde{T}) C_S(\tilde{T}) \frac{\partial \tilde{T}}{\partial t} - d_S \nabla_t \cdot (K_S(\tilde{T}) \nabla_t \tilde{T}) - K_S(\tilde{T}) \frac{\partial T}{\partial z}\bigg|_{z=0}^{d_S} = d_S Q(\tilde{T}) \tag{10}$$

where ∇_t is the tangential gradient operator and $\tilde{T} = \frac{1}{d_S}\int_0^{d_S} T\, dz$. Here d_S is the superconducting layer thickness and $z = 0$ and $z = d_S$ locate the bottom and top surfaces of the superconducting layer, denoted as Γ^- and Γ^+. In performing the integration, the parameters are considered functions independent of z. The boundary term on the LHS of equation (10) is equal to the difference of the normal heat fluxes on the upper and lower surfaces of the superconducting layer, which are approximated as the normal fluxes flowing across the silver and buffer layers, respectively.

The normal heat fluxes across the silver layer and buffer layers are modeled by thin-layer thermal contact resistance type identity pair boundary conditions. These boundary conditions are imposed on the identity boundary pairs between the lower surface of the top copper stabilizer and the top surface of the superconducting layer, and between the bottom surface of the superconducting layer and the top surface of the substrate. The identity pair boundary conditions also couple the 2D thermal physics of the superconducting layer to the 3D physics of the copper stabilizer and substrate. By using these boundary conditions, the boundary terms in equation (10) can then be rewritten as

$$F^+ \equiv -K_S(\tilde{T}) \frac{\partial T}{\partial z}\bigg|_{\Gamma^+} \approx K_{cu} \nabla T \cdot \mathbf{n}\big|_{\Gamma_{cu}^-} = -\frac{K_a}{d_a}(T_{cu}^- - T^+) \tag{11}$$

$$F^- \equiv K_S(\tilde{T}) \frac{\partial T}{\partial z}\bigg|_{\Gamma^-} \approx K_{ni} \nabla T \cdot \mathbf{n}\big|_{\Gamma_{ni}^+} = -\frac{K_b}{d_b}(T_{ni}^+ - T^-) \tag{12}$$

where F^+ and F^- represent the normal heat fluxes flowing across the top and bottom surfaces of the superconducting layer. The subscripts a and b represent the silver layer and buffer layers, d_a and d_b represent the thicknesses of the silver layer and buffer layers, T_{cu}^- and Γ_{cu}^- represent the temperature and boundary on the lower surface of the top stabilizer while T_{ni}^+ and Γ_{ni}^+ are on the upper surface of the substrate, and T^+ and T^- denote the temperatures on the upper and lower surfaces of the superconducting layer. As a result, the tangential 2D thermal equation (10) is approximated in weak boundary form as

$$d_S \rho_S(\tilde{T}) C_S(\tilde{T}) \frac{\partial \tilde{T}}{\partial t} - d_S \nabla_t \cdot (K_S(\tilde{T}) \nabla_t \tilde{T}) = d_S Q(\tilde{T}) + \frac{K_a}{d_a}(T_{cu}^- - T^+) + \frac{K_b}{d_b}(T_{ni}^+ - T^-). \tag{13}$$

Due to the 2D approximation of the superconducting layer, T^+ and T^- are actually the same and equal to $\tilde{T}$. Numerical simulations show that the temperature gradient which

appears in a full 3D simulation is an important factor affecting simulation accuracy. To account for the temperature gradient within the superconducting, using $\tilde{T} = (T^+ + T^-)/2$ as an approximation of $\tilde{T}$, and equation (13) as a hint, the approximations of the higher temperature T^+ and lower temperature T^- are written as

$$T^+ = 2\tilde{T} - T^- \tag{14}$$

$$T^- = \frac{\left\lfloor 2\tilde{T} + \left(\frac{K_a}{d_a}(2\tilde{T} - T_{cu}^-) - d_S Q_S \right) \frac{d_S}{K_S} \right\rfloor}{\left(2 + \frac{K_a}{d_a}\frac{d_S}{K_S} \right)}. \tag{15}$$

This thermal correction reproduces the temperature gradient across the thickness of a 3D superconducting layer and greatly improves the accuracy of the reduced dimensional approximation. Section 3 will give some details about the simulation accuracies and errors.

To further account for the in-plane thermal physics along the silver layer and buffer layers, surface heat equations plus heat sources are imposed, in addition to the normal heat fluxes F^+ and F^-, as interior boundary conditions on the top copper stabilizer lower surface and the substrate upper surface:

$$\begin{aligned} -K_{cu}\nabla T \cdot \mathbf{n}\big|_{\Gamma_{cu}^-} &= F^+ \\ &+ d_a \sigma_a \left[\left(\frac{(V_{cu}^- - V^+)}{d_a} \right)^2 + \left(\nabla_t V_{cu}^- \right)^2 \right] \\ &- d_a \rho_a C_a \frac{\partial T}{\partial t} + d_a \nabla_t \cdot (K_a(T) \nabla_t T) \end{aligned} \tag{16}$$

$$\begin{aligned} -K_{ni}\nabla T \cdot \mathbf{n}\big|_{\Gamma_{ni}^+} &= F^- \\ &+ d_b \sigma_b \left[\left(\frac{(V_{ni}^+ - V^-)}{d_b} \right)^2 + \left(\nabla_t V_{ni}^+ \right)^2 \right] \\ &- d_b \rho_b C_b \frac{\partial T}{\partial t} + d_b \nabla_t \cdot (K_b(T) \nabla_t T). \end{aligned} \tag{17}$$

The square bracketed terms are the normal and tangential Joule heating on the silver layer and buffer layers. Here, V_{cu}^- and V_{ni}^+ are the electric potential on the top stabilizer lower surface and substrate upper surface, and V^+ and V^- are the electric potentials on the upper and lower surfaces of the superconducting layer.

A 2D tangential electrical equation for the superconducting layer is obtained using the same approach used to derive the 2D tangential thermal equation. The planar current flowing along the silver layer and buffer layers is neglected and the currents flowing across the thickness of these layers in the normal direction are approximated by contact resistance type identity pair boundary conditions similar to equations (11) and (12) as:

$$\begin{aligned} -\sigma_S \nabla V \cdot \mathbf{n}\big|_{\Gamma^+} &\approx \sigma_{cu} \nabla V \cdot \mathbf{n}\big|_{\Gamma_{cu}^-} \\ &= -\frac{\sigma_a}{d_a}(V_{cu}^- - V^+) \end{aligned} \tag{18}$$

$$\begin{aligned} -\sigma_S \nabla V \cdot \mathbf{n}\big|_{\Gamma^-} &\approx \sigma_{ni} \nabla V \cdot \mathbf{n}\big|_{\Gamma_{ni}^+} \\ &= -\frac{\sigma_b}{d_b}(V_{ni}^+ - V^-). \end{aligned} \tag{19}$$

Analogous to the derivation of the tangential thermal equation, a 2D tangential electrical equation results:

$$\begin{aligned} d_S \nabla_t \cdot (-\sigma_S(\tilde{T}) \nabla_t \tilde{V}) &= \frac{\sigma_a}{d_a}(V_{cu}^- - V^+) \\ &+ \frac{\sigma_b}{d_b}(V_{ni}^+ - V^-) \end{aligned} \tag{20}$$

where $\tilde{V} = \frac{1}{d_y}\int_0^{d_y} V\, dz$. Due to the 2D approximation of the superconducting layer, however, the electric potentials V^+ and V^- are identical and equal to $\tilde{V}$. In contrast, there is a potential differential between the top and bottom surfaces in 3D superconducting layers. Physically, the potentials across the silver layer and buffer layers must match over the normal zone region since there is minimal or zero current flowing across the highly resistive normal zone of the superconducting layer. Using a full 3D simulation result as a hint, a potential difference is created on the 2D superconducting layer over the normal zone through

$$V^+ = \begin{cases} V_{cu}^- \text{ if } \sigma_S > 1e-4\ S/m \text{ and } \sigma_a \le \sigma_b \\ \tilde{V} \quad \text{else} \end{cases} \tag{21}$$

$$V^- = \begin{cases} V_{ni}^+ \text{ if } \sigma_S > 1e-4\ S/m \text{ and } \sigma_a > \sigma_b \\ \tilde{V} \quad \text{else}. \end{cases} \tag{22}$$

This potential correction eliminates any otherwise artificial current flowing over the normal zone. The cut-off value of 10^{-4} is chosen

to be larger than but close to the normal state conductivity of the superconductor.

The magnetic field generated by the current flowing in the 3D domains such as the stabilizer and the substrate is accounted for by the magnetic potential equation (4). The magnetic field generated by the current flowing in the superconducting layer is taken into account by using the surface current type identity pair boundary condition imposed on the identity pair pairing the top stabilizer lower surface and the substrate top surface. The generated magnetic field is coupled to the superconducting layer via the $J_c(T,\mathbf{B})$ equation (8).

3. Validation and Results

Analytical solution for a full nonlinear superconducting tape model without simplification is nearly impossible to obtain. Thus, the mixed-dimensional model, denoted hereafter as 3D/2D model, is validated by numerical and experimental validations. Experimental validation, though the most trustable way to verify a model, is limited to the observation of measurable quantities such as voltage and temperature on the tape surface. Numerical validation based on an equivalent 3D computational model allows the observation of the inner details within a tape model.

For numerical validation, short 3D/2D and partial- and full-3D tape models of 5 mm long and 0.5 mm wide are used. A full-3D model meshes all layers including the superconducting, silver and buffer layers in 3D while a partial-3D model approximates the silver and buffer layers with interior boundary conditions. Figure 3 illustrates the impact of the thermal corrective equations (14) and (15) on the temperature distribution and accuracy of the 3D/2D model. Figure 3(a) shows a snapshot of the temperature distribution from a partial-3D model. Figure 3(b) is from a 3D/2D model with thermal correction, and Figure 3(c) is the same 3D/2D model but without the thermal correction. All three cases are taken at the same time at t = 5 x 10^{-4} s during quenches. As can be seen by comparing Figure 3(a) and 3(b), the thermal correction reproduced the temperature gradient across the 3D superconductor (YBCO) layer of the partial-3D model in the 3D/2D model. It also greatly improves the accuracies in the position of the T_c front and the temperature. See the caption in Figure 3 for the exact values of the position, temperature and error. In contrast, the accuracies of the 3D/2D model without the thermal correction, as shown in Figure 3(c), are poor. The thermal and potential corrections on the superconducting layer significantly improve the accuracy of the 3D/2D model. The maximum numerical error is reduced from 15.8 % without corrections to 0.7 % with corrections, as compared to the corresponding partial-3D model in NZPV and peak temperature. Implementing all the thermal and electrical equations from section 2 reduces the maximum numerical error of the 3D/2D models from 26% to less than 3.8%, as compared to the results generated by a corresponding full-3D model.

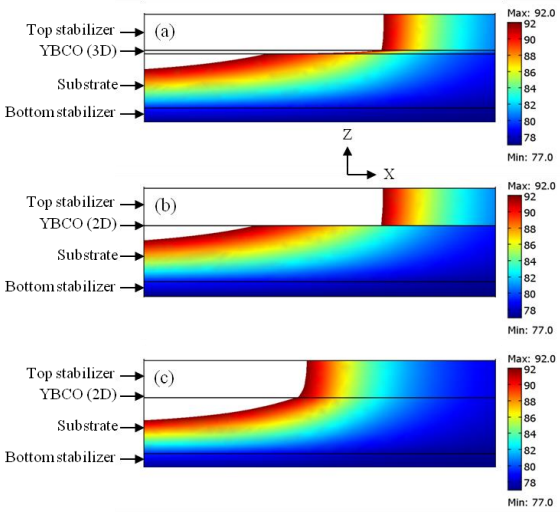

Figure 3. Snapshots of T(x, z) during a quench in a surround-stabilizer tape. (a) A partial-3D tape model. The T_c front at the copper-superconductor (YBCO) interface is located at x = 1.76 mm and the peak temperature T_{max} = 122.2 K. (b) A mixed-dimensional 3D/2D model with thermal correction which reproduces the temperature gradient across the superconductor layer. The T_c front is located at x = 1.77 mm (error = 0.4%) and T_{max} = 121.8 K (error = 0.3%). (c) The same mixed-dimensional 3D/2D model as in (b) but without the thermal correction. The T_c front is located at x = 1.52 mm (error = 13.7 %) and T_{max} = 106.1 K (error = 13.2%).

Besides NZPV and temperature, comparisons of other quantities are also used to gauge the accuracy of the 3D/2D model as compared to its full 3D model counterpart. As an example, Figure 4 compares the Joule heating during a quench versus longitudinal length profiles

obtained from a 3D/2D tape, as shown in Figure 4(a), and a full-3D counterpart, as shown in Figure 4(b). Graphs of the same legend and color represent the Joule heating measured from the same particular layer in both tapes. As can be seen, the two profiles match each other very well. Note that during a quench, most of the Joule heating occurs at the top copper stabilizer (Q_cu, brown lines) over the normal zone where the Joule heating on the superconducting layer (Q_y, red lines) drops sharply to near zero.

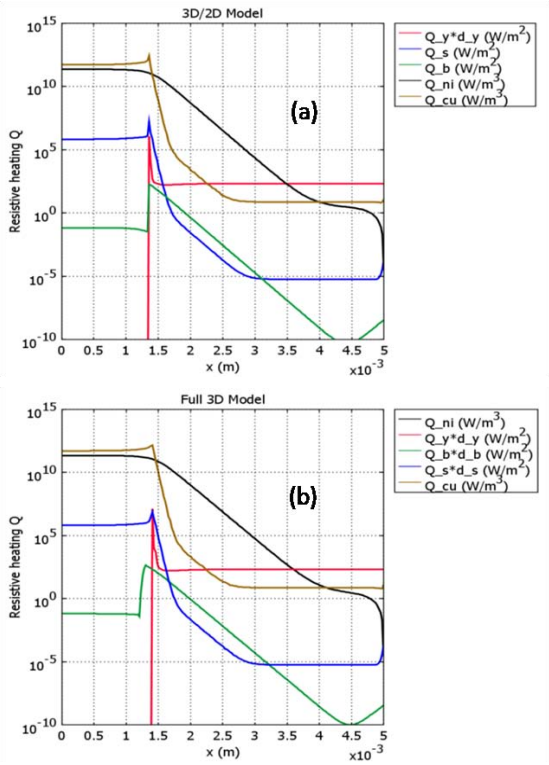

Figure 4. Comparison of Joule heating (in surface and volume densities) versus longitudinal length profiles obtained from 3D/2D (a) and full-3D models (b). Red lines (Q_y) are Joule heating measured from the superconducting layer. Brown lines (Q_cu) are from top copper stabilizer, black lines (Q_ni) are from substrate, blue lines (Q_s) are from silver layer while green lines (Q_b) are from buffer layer.

The experimental validation uses readily available experimental results reported in [3]. A 90 mm x 2 mm quarter-size 3D/2D tape model as shown schematically in Figure 1 is used in simulation. Temperature-dependent material properties are obtained from the COMSOL material library, from in-house measurements and published data. There are a number of unknown parameters needed to be estimated in the simulations. The main unknown parameters are the thickness of the side stabilizer, the power indices n, the heat transfer coefficients at the base and end of the tape, the effective thermal conductivity of the heater, and thermal and electrical conductivities of the buffer layers. A possible set of temperature independent values of the unknown parameters are first chosen within the limits of available material property data and then refined by comparing the simulation results to the experimental results. This is repeated until the NZPVs and the voltage and temperature profiles generated from the simulations approach the experimental results.

Figure 5 shows the NZPVs from the simulations and experimental data corresponding to different J_a/J_{co} ratios under different operating temperatures. In these simulations, magnetic field calculation is not considered by excluding equation (4) and setting $J_c(T,\mathbf{B}) = J_c(T)$. The NZPVs from the simulations using the 3D/2D tape models are in good agreement with the experimental data; all errors are within 9%.

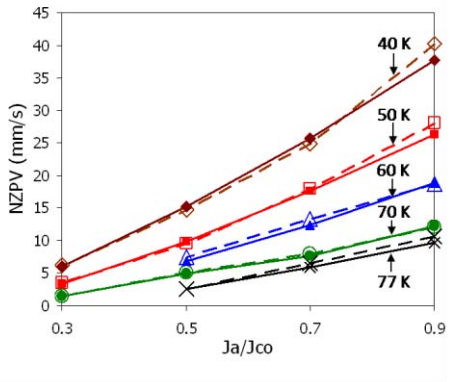

Figure 5. Comparison of NZPVs between experimental results from [3] (solid lines) and simulation results (dashed lines) on a 90 mm long half-length surround-stabilizer tape. The horizontal axis represents the ratio of the applied current density to critical current density at the operating temperature. Graphs from top to bottom correspond to cases with operating temperatures of 40 K, 50 K, 60 K, 70 K and 77 K.

Figure 6 gives another example showing that the 3D/2D model is capable of predicting accurately the physical quench behavior of a real case CC tape. Figure 6(a) shows the voltage versus time profile measured from experimental tape corresponding to the $J/J_c = 0.5$ and $T_o = 70$

K case in Figure 5. Figure 6(b) shows the same profile obtained from a 3D/2D model. Observe that the two profiles match each other well. The nonlinear segment of a voltage (difference) curve reflects the occurrence of current sharing in the region bounded by the two voltage taps. Within the current sharing region, the superconductor becomes resistivity and current redistributes from the superconducting layer to the stabilizer. The nearly linear segment of the curve signifies that the current is flowing completely on the stabilizer. More details about the 3D/2D model and its validation results can be found in [4].

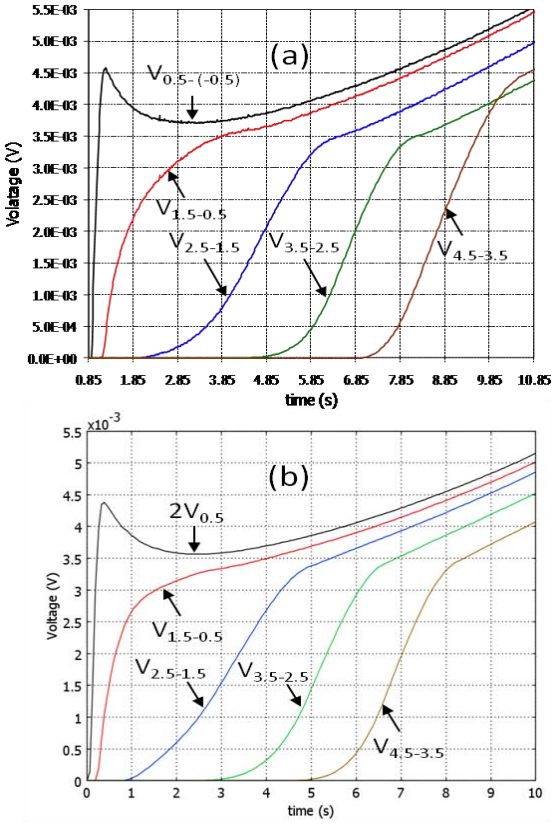

Figure 6. (a) Voltage versus time obtained experimentally as reported in [3]. In this case, J/J_c = 0.5 and T_o = 70 K. The voltage $V_{3.5-2.5}$ is the difference between the voltages measured at the voltage taps $V_{3.5}$ and $V_{2.5}$ as defined in Figure 1. The voltage tap $V_{-0.5}$ used for the voltage differential $V_{0.5-(-0.5)}$ is located at x = -0.5 cm on the surface of the experimental tape. Note that the heater pulse starts at t = 0.85 s, so the time scale is shifted to match the time-axis in (b). (b) Voltage versus time obtained from simulations of a 90 mm x 2 mm quarter-size surround-stabilizer tape, corresponding to the same conditions and voltage tap definitions as in (a).

4. Conclusions

The 3D/2D model allows the study of micrometer-scale quench propagation details within a HTS CC tape. The mixed-dimensional modeling approach renders the FE meshing independent of the thicknesses of the laminated thin layers. This effectively addresses the problematic high aspect ratio FE modeling issues. The 3D/2D model saves more than three times FE degrees of freedom and computes efficiently at a speed at least eight times faster than its full-3D counterparts. This speed efficiency is due partly to the reduction in FE unknowns and partly to the decomposition of the numerical domain into separated, easier-to-compute domains of vastly different material properties by the interior boundary conditions.

Validation results show that a laboratory size 3D/2D model is capable of reproducing accurately the detailed physical quench phenomena observed experimentally.

5. References

[1] E. H. Brandt, "Thin superconductors in a perpendicular magnetic AC field - general formulation and strip geometry," *Physical Review B*, vol. 49, pp. 9024-9040, Apr 1994.

[2] R. Brambilla, *et al.*, "Integral equations for the current density in thin conductors and their solution by the finite-element method," *Superconductor Science & Technology*, vol. 21, p. 105008, Oct 2008.

[3] X. Wang, *et al.*, "Near-adiabatic quench experiments on short $YBa_2Cu_3O_{7-\delta}$ coated conductors," *Journal of Applied Physics*, vol. 101, p. 053904, Mar 2007.

[4] W.K. Chan, *et al.*, " Three-dimensional Micrometer-scale Modeling of Quenching in High Aspect Ratio $YBa_2Cu_3O_{7-\delta}$ Coated Conductor Tapes. Part I: Model Development and Validation," *IEEE Transactions on Applied Superconductivity*, in press.

6. Acknowledgements

The authors thank X. R. Wang for the experimental data used for the validation. This work is supported in part by the Air Force Research Laboratory.